Experimental and Numerical Investigation of Alkali Silica Reaction in Nuclear Reactors

Grant No.: NRC-HQ-60-14-G-0010

Oct. 2014 - Dec. 2017
($703,197)

Final (Public) Summary Report*
December 2017

Principal Investigator
Victor E. Saouma
University of Colorado, Boulder

NRC Technical Contact
Madhumita Sircar

* Synthesis of Confidential Reports:

1-A: *Design of an AAR Prone Concrete Mix for Large Scale Testing*
1-B: *AAR Expansion; Effect of Reinforcement, Specimen Type, and Temperature*
1-C: *Effect of AAR on Shear Strength of Panels*
2: *Diagnosis & Prognosis of AAR in Existing Structures*
3-a: *Risk Based Assessment of the Effect of AAR on Shear Walls Strength*
3-b: *Probabilistic Based Nonlinear Seismic Analysis of Nuclear Containment Vessel Structures with AAR*

NOTES

This report provides a synthesis of the following confidential documents submitted to the NRC:

1-A: Design of an AAR-Prone Concrete Mix for Large-Scale Testing (93 pages).
1-B: AAR Expansion; Effect of Reinforcement, Specimen Type, and Temperature (123 pages).
1-C: Effect of AAR on the Shear Strength of Panels (90 pages).
2: Diagnosis & Prognosis of AAR in Existing Structures (191 pages).
3-A: Risk-Based Assessment of the Effect of AAR on Shear Wall Strength (25 pages).
3-B: Probabilistic-Based Nonlinear Seismic Analysis of Nuclear Containment Vessel Structures with AAR (216 pages).

Disclaimer: The views and opinions expressed in this report are those of the author and do not necessarily reflect the official position of the Nuclear Regulatory Commission. Examples of analysis performed within this report are only examples. They should not be utilized in real-world analytic products as they are based only on very limited and dated open source information.

Contents

List of Figures

List of Tables

1 Introduction

1.1 Objectives and Main Conclusion

1 This project has addressed the two most important questions raised by a nuclear containment vessel structure (NCVS) subjected to Alkali-Aggregate Reaction (AAR):

1. How fast will the reaction evolve, and what is the anticipated maximum expansion?
2. Is the resilience (i.e. ability to safely withstand an earthquake) affected and, if so, by how much?

Those are critical question the *beyond 60* possible life extension of NCVS.

2 It will be shown herein that based on the tests ("high" expansion of $\sim 0.6\%$) and analyses ("moderate" expansion of $\sim 0.3\%$) performed, a $\sim$20% degradation is likely to occur in both cases.

1.2 Tasks

3 In recognition of the fact that this is a complex coupled problem requiring expertise in both materials (understanding, testing) and structures (ability to conduct credible analyses), a holistic approach has been implemented to complete the following tasks:

Task 1: Two subtasks are summarized in the reports:

- **1-A: Mix Design** Design a concrete mix (with locally available aggregates) that will expand by approximately 0.5% in 6 months, has a compressive strength of around 4,500 psi, a 3" slump and low air content.
- **1-B Expansion Monitoring:** Cast not only 16 shear specimens but many others as well[1] (such as specimens with various uniaxial, biaxial or triaxial reinforcements), cure them under controlled conditions and assess both expansion and crack indices.
- **1-C Shear tests*:** assess shear strength degradation of plain and structural concrete subjected to AAR.

Task 2*: Develop a diagnosis and prognosis tool based on the accelerated test in order to assess residual expansion over time. More specifically: a) Diagnosis to estimate the degree of reaction in concrete along with the corresponding expansion; b) Prognosis to predict future and ultimate ASR expansion; and c) provide results in a format suitable for proper finite element simulation.

Task 3: Numerical simulations using our Merlin finite element code and its constitutive model for AAR, which has been adopted by many researchers and practitioners. Two subtasks are included:

- **3-A: Risk-Based Assessment of a shear wall** subjected to a reverse cyclic load and tested at the University of Toronto. These steps were carried out within the scope of an ASCET round robin.
- **3-B Impact of AAR on Seismic Response*** of an NCVS.

Each of these tasks will be summarized separately. Those identified by an * directly address the scope of the project, others are supportive tasks.

1.3 PI Credentials

4 Victor Saouma is a Professor of Civil Engineering at the University of Colorado in Boulder; Chair of RILEM's Committee on the Prognosis of deterioration and loss of serviceability in structures affected by alkali-silica reactions; past President of FraMCoS (Fracture Mechanics of Concrete); conducted AAR related research for the Swiss federal dam safety agency, the Tokyo Electric Power Company (TEPCO), the Oak

[1] Note: The contract called for 8 specimens, with no monitoring of additional specimens.

Ridge National Laboratory; Member of the Materials Aging and Degradation (MAaD) External Review Committee (ORNL, Light Water Reactor Sustainability R&D Program); past member of the Expanded Proactive Materials Degradation Analysis Expert Panel (PMDA) for concrete in nuclear reactors; Reviewer of the French research program MACENA (associated with VeRCoRs); recently published an EPRI report on the numerical modeling of NCVS; is about to launch a major 3-year research program on AAR for the Bureau of Reclamation; published a book on Numerical Modeling of AAR; has published over 30 papers on AAR, chloride diffusion, Seismic Analysis and Stochastic Analyses (his paper on an AAR constitutive model is probably the most widely copied and cited); has pioneered dynamic testing (real-time hybrid simulation); is also the Managing Partner of a recently formed consulting company X-Elastica.

2 Research Tasks

2.1 Task 1: Shear Strength Degradation

2.1.1 Task 1-A: Concrete Mix Design

5 Assessment of the impact of AAR through a laboratory testing campaign hinges on our ability to replicate a mix design that is representative of the one used in NCVS. For starters, reactive aggregates had to be identified in Colorado, then the concrete mix design had to be developed.

6 Two sources of aggregates were first identified, and expansion mortar tests were performed on variously-sized aggregates, Fig. 1. Both sources yielded highly reactive aggregates, and one was selected.

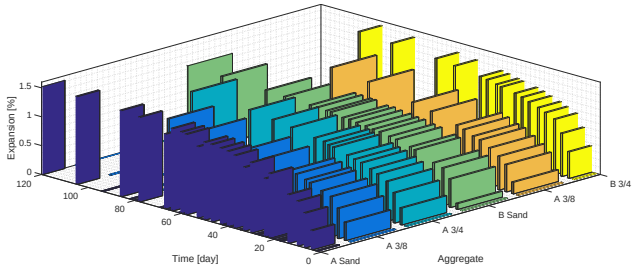

Figure 1: Expansion of mortar bar tests

7 Following the selection of an aggregate source, a concrete mix design with: a minimum compressive strength of 4,000 psi [27.6 MPa], a slump[2] of 5 in. [12.7 cm], an air content set at 3%, and, most importantly, the expansion target for reactive samples set at a relatively high 0.5% (to be reached within approximately 6 months under 95% RH and 38°C temperature) had to be designed.

8 In order to enhance the reaction, cement with a high natural alkalinity was selected and then the alkalinity was further raised by adding sodium hydroxide.

9 Control specimens used the same reactive aggregates[3]; however, they were (successfully) enriched with lithium, which inhibited the reaction.

10 Throughout this task, ASTM standards were strictly respected, Table 1.

[2]The slump value is slightly higher than normal; however, most specimens had to receive closely-spaced reinforcements and moreover no superplasticizer was used so as not to interfere with either the sodium hydroxide or lithium, which were introduced to enhance or inhibit the AAR reaction.

[3]It is the P.I. firm conviction that using a different non-reactive aggregate, or fly ash, can be very misleading when interpreting results.

Table 1: Standards used for aggregate and concrete testing programs

Aggregate Tests	Standard	Concrete Test	Standard
Coarse aggregate relative density	ASTM C127	Slump	ASTM C173
Fine aggregate relative density	ASTM C128	Unit Weight	ASTM C138
Coarse aggregate bulk density	ASTM C29	Air Content	ASTM C231
Fineness modulus/gradation	ASTM C136	Temperature	ASTM C1064
Moisture content	ASTM C566	Compressive Strength	ASTM C39
		ASR Expansion	Modified ASTM C1293

11 A petrographic analysis of the concrete prism and two mortar bars was conducted to verify that the expansion observed was indeed a result of expansive gels due to ASR. The reactive aggregates were identified as a reactive mix of porous and semi-porous flint-like grains, metamorphic, sedimentary and magmatic rock types.

12 Average expansions of the cast concrete are shown below in Fig. 4(a) for specimens stored in the fog room (average RH 95%, T=38°C)

2.1.2 Task 1-B: Expansion Monitoring

13 16 concrete panels were to be cast for testing once sufficient expansion had occurred. It was thus decided to pour a total of 37 additional specimens in order to monitor expansion under different conditions (10 6x6x14", 12 4x4x16" prisms, and 15 14x14x14" blocks). These various specimens were stored under different temperatures, and some were fitted with strain and temperature gages.

14 In an attempt to further elucidate the impact of isotropic or anisotropic reinforcement on expansion, the 14" x 14" x 14" blocks were assigned different reinforcement ratios ρ using #3 or # 4 steel reinforcement, Fig. 2.

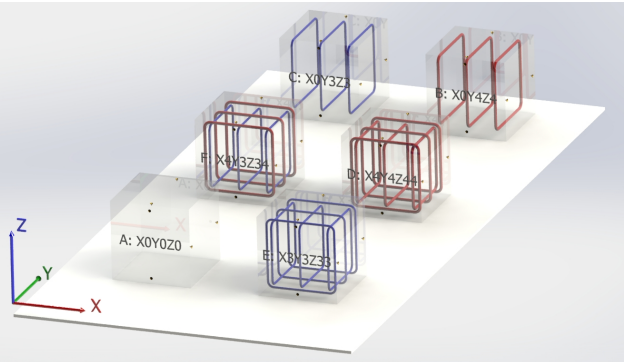

Figure 2: 14" × 14" × 14" blocks with various reinforcements

15 The fog room arrangement for specimens stored at 95°F and ∼ 90% RH was carefully planned (due to limited size), Fig. 3(a).

16 The leaching (caused by a difference in alkalinity between specimen and ambient air) of alkalinity from the concrete was a major potential problem. It was addressed by wrapping specimens in burlap and continuously wetting them with a 1M aqueous sodium hydroxide (NaOH) solution, Fig. 3(b).

17 A total of 147 expansion readings were recorded periodically, stored in a database and then analyzed. The expansion readings were continuously recorded, Fig. 4(a).

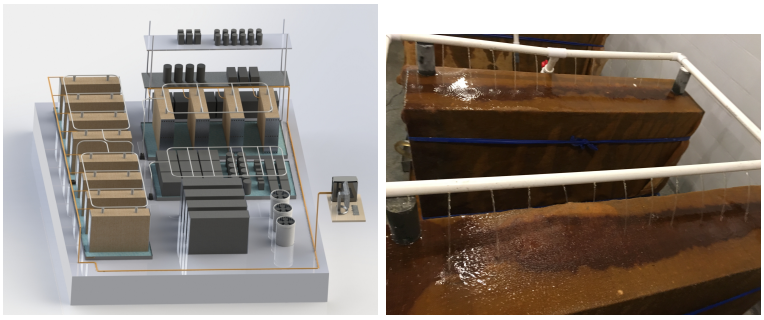

(a) Installation of reactive and non-reactive shear specimens, blocks, prisms and cylinders in the fog room

(b) Sprinkler system wetting the burlap-wrapped shear specimen

Figure 3: Storage of specimens

Likewise, some 160 crack index readings were recorded at age 520 days (with 0.005" resolution), Fig. 4(b).

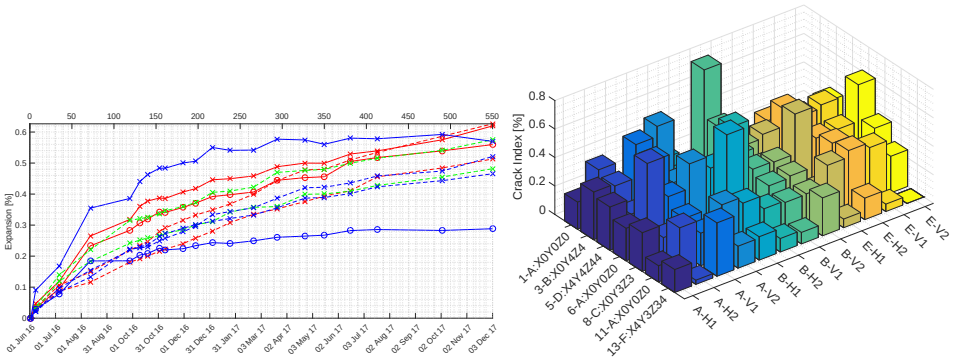

(a) Expansions of all $6 \times 6 \times 14$-inch prisms (P14)

(b) Crack Indices for Cubes

Figure 4: Examples of recorded measurements

The extensive (multi-variable) database was then analyzed and various effects were quantified, Fig. 5.

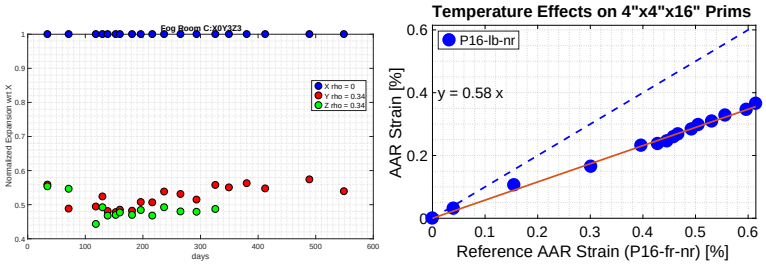

(a) Normalized expansions for various reinforcement ratios

(b) Effect of Temperature on Prisms

Figure 5: Example of an expansion measurement analysis

2.1.3 Task 1-C*: Shear Tests

20 This is one of the two most important tasks: the experimental assessment of the impact of AAR on the shear strength of both plain and reinforced concrete. The former is a material characterization, while the latter involves a structural characterization.

21 The shear strength assessment should not be "corrupted" by flexural stresses[4]. On the other hand, perfect shear tests are mechanically impossible, yet they may be closely approximated through a complex set-up.

22 The test concept is illustrated in Fig. 6(a). A 10x30x40-inch concrete block (plain or reinforced) is first placed inside a stiff cage, or "shear box" (shown in blue) and is then subjected to: a) a constant lateral confinement force (simulating the vertical stress at the simulated location); and b) two opposing vertical forces applied through eccentrically placed pads (shown in black), thus the vertical forces are ultimately imposing shear forces. As a result, a diagonal crack will develop within the (red) band. Finally, the shear box is placed within the confines of a one million-pound (previously calibrated) MTS testing machine, Fig. 6(b).

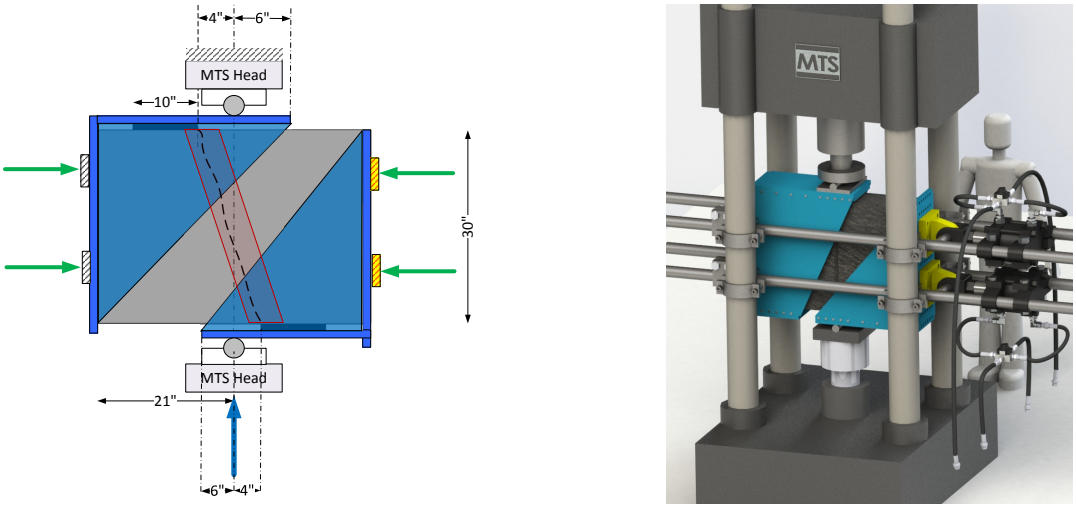

(a) Concrete panel inside the shear box.

(b) Shear box inside the testing machine

Figure 6: Experimental Set-up

23 For the structural assessment, the panels must be correlated with an actual NCVS within the limits of testing constraints. Conceptually speaking, the model may be viewed as "extracted" from the NCVS, rotated 90 degrees and then inserted into the load frame for testing, Fig. 7.

24 It is important to note that the circumferential reinforcement (shown in blue) corresponds to the short transverse steel rods in the specimen, while the vertical (red) rods correspond to the axial reinforcements in the specimen.

25 Prior to testing, the 28-day compressive strength was correlated with the one-year tensile splitting strength, revealing noticeable deterioration in the latter for the reactive concrete, Fig. 8.

26 Six groups of specimens (labeled A through H) were tested, Fig. 9. Most specimens where subjected to a

[4]For this reason, shear strength cannot reliably be assessed using beams.

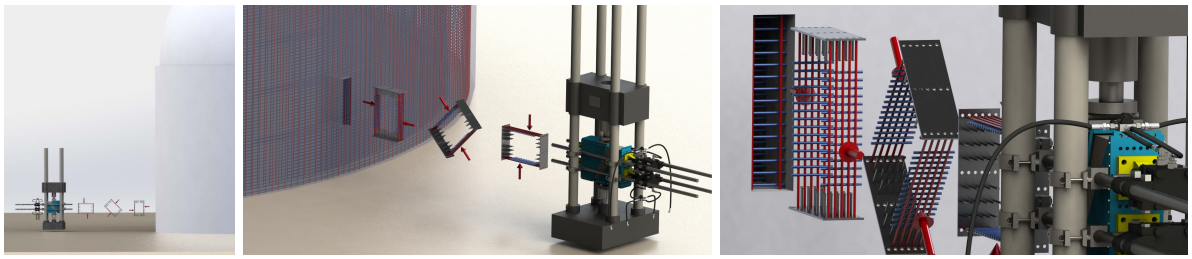

Figure 7: Interaction between model and specimens

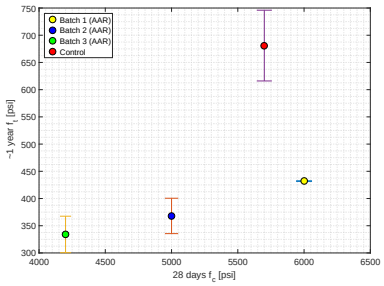

Figure 8: Compressive strength *vs.* tensile splitting strength

"baseline" confining force (based on the concrete weight above the level considered), while others were tested at lower or higher values to assess their impact on strength. The test matrix can be better visualized (and understood) by means of Fig. 9.

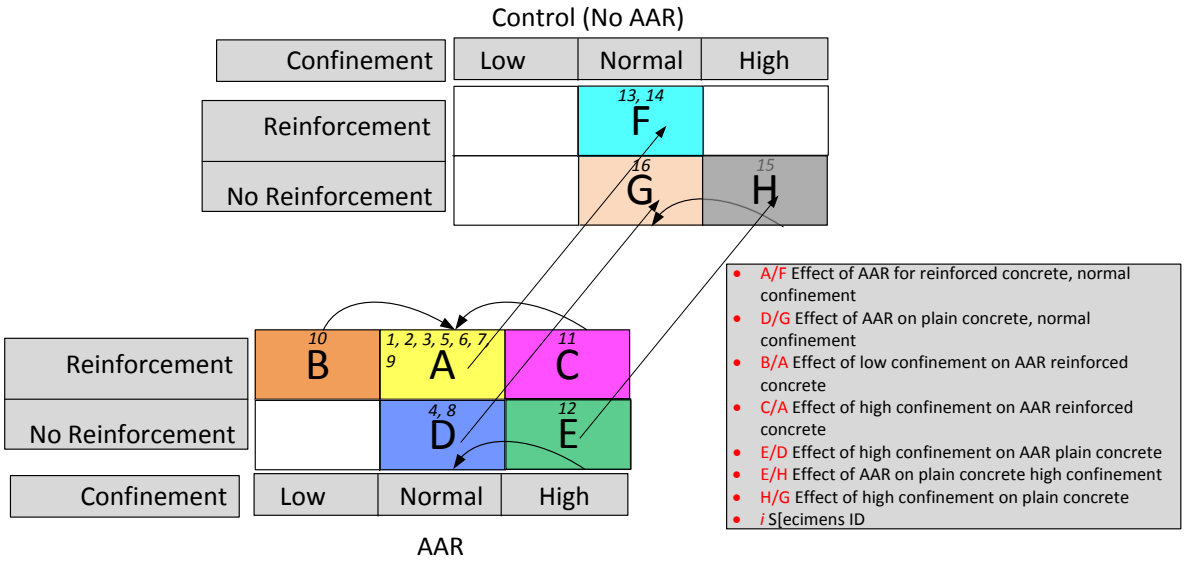

Figure 9: Test Matrix

For the previously defined test matrix, the 7 following questions were investigated:

Effect of AAR on material and structural responses:

1. **A-F** What is the effect of AAR on reinforced concrete (structure) subjected to a base confinement?

2. **D-G** What is the effect of AAR on plain concrete (material) subjected to a base confinement?
3. **E-H** What is the effect of AAR on plain concrete (material) subjected to high confinement?

Effect of Confinements under various scenarios. This will nullify (to some extent) the impact of the selected baseline normal traction and moreover confirm the result of whether a higher confinement yields a higher failure shear force:

4. **B-A** What is the effect of low confinement on reinforced concrete with AAR?
5. **C-A** What is the effect of high confinement on reinforced concrete with AAR?
6. **E-D** What is the effect of high confinement on plain concrete with AAR?
7. **H-G** What is the effect of high confinement on plain concrete without AAR?

[28] At the time of testing, the AAR expansion was about 0.6%, Fig. 4(a).

[29] Fig. 10(a) summarizes all of the 16 individual experimental and numerical (to be discussed further below) results in a single diagram. In absolute value terms, these results are relatively insignificant, as they would need to be normalized (as dictated by the questions raised above). Fig. 10(b) shows the normalized means (when more than one data point exists) with respect to the reference means (as indicated in Fig. 9).

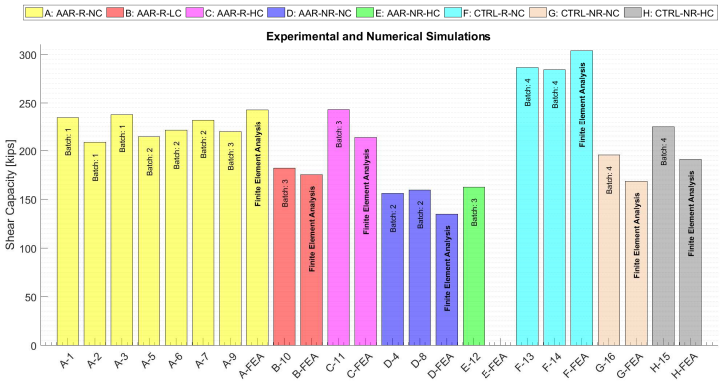

(a) Raw results

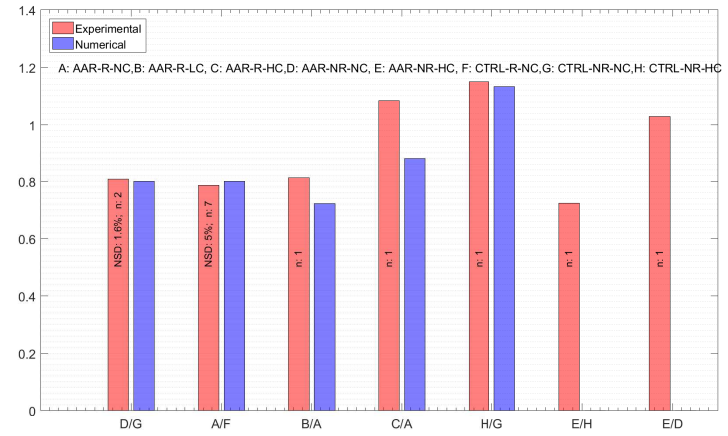

(b) Normalized experimental and numerical results

Figure 10: Experimental and numerical results

30 A statistical summary of these test results is provided in Table 2, along with an attempt at normalizing shear forces with $\sqrt{f'_c}$, f'_c and f'_t (let's recall herein that the ACI shear strength equation is a function of $\sqrt{f'_c}$).

Table 2: Statistical analysis of results

	$P1$	$P2$	$P3$	$P4$
	Exp. P_{max}	$P1/\sqrt{f'_c}$	$P1/f'_c$	$P1/f_t$
A, B, C, D, E Cumulative				
Mean	**202.64**	91.11	41.15	549.20
std/Mean	**16%**	16%	19%	22%
F, G, H Cumulative				
Mean	**247.65**	103.73	43.45	364.19
std/Mean	**18%**	18%	18%	18%

31 A finite element simulation of the tests was performed using the code named Merlin. The numerically computed load-displacement curves are shown in Figs. 11(a) and 11(b), while the corresponding experimental results are simply presented as an asymptotic horizontal peak value[5]. Fig. 11(c) shows the extent of internal cracking, corresponding to various points along the load-displacement curve.

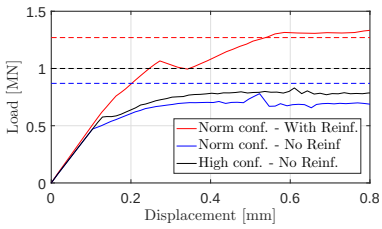

(a) Control specimens

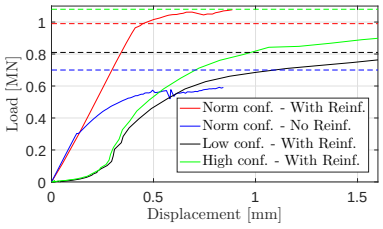

(b) AAR

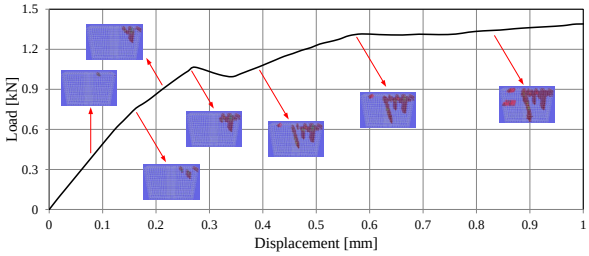

(c) Computed internal cracking, in terms of the load-displacement curve

Figure 11: FEA simulations.

32 Based on the above, the following observations can be proposed:

1. Test results are remarkably close within a given group. The normalized standard deviations for series A, D and F (where more than one test is available) are 5.0, 2.0 and 0.58 percent, respectively. This finding reinforces the reliability of our test program.

[5]Experimentally speaking, the measured actuator stroke included substantial elastic deformation of the blue cage housing the specimen, Fig. 6(a).

2. The finite element simulations accurately replicated the experimental results. Hence, a similar simulation could assess with good reliability the shear degradation corresponding to different levels of AAR expansion.
3. The AAR causes a ≈20% reduction in shear strength for reinforced concrete specimens (i.e. structural effect) under base confinement; A/F.
4. The AAR causes a ≈20% reduction in shear strength for non-reinforced concrete specimens (i.e. material effect) under base confinement; D/G.
5. The AAR causes a ≈20% reduction in shear strength for non-reinforced concrete specimens (i.e. material effect) under high confinement; E/H.
6. A reduction in confinement for reinforced concrete panels with AAR resulted in a ≈20% reduction in shear strength; B/A.
7. An increase in confinement for reinforced concrete panels with AAR resulted in a ≈10% increase in shear strength; C/A. This effect is not accurately replicated numerically.
8. An increase in confinement for non-reinforced concrete panels with AAR resulted in an ≈10%increase in shear strength of; E/D.
9. An increase in confinement for non-reinforced concrete panels without AAR resulted in a ≈20% increase in shear strength; H/G.
10. When experimental shear strength $P1$ is normalized with respect to $\sqrt{f'_c}$, f'_c and f_t ($P2$, $P3$, and $P4$, respectively) for all test series, see Table 2, the lowest normalized standard deviations are associated with $P1$ and $P2$. Non-reactive concrete exhibits slightly higher values (18% vs. 16%); however, this effect may be due to the limited number of data points (4 instead of 12).
11. The shear strength degradation of ≈20% is less than the splitting tensile strength decrease (≈50%), Fig. 8.

All these results had been anticipated but, prior to this present research program, were not yet quantifiable.

2.2 Task 2: Prognosis for Future Expansion/RILEM

A RILEM Committee chaired by the P.I. is dedicated to this task. The roughly 36-member committee contains all the renowned leaders in this specific field of concern.

Working Groups:

WG1: - Diagnosis and prognosis of AAS in existing structures Prognosis The report will address: 1) Diagnoses based on petrographic and microscopic interpretation to estimate the degree of past expansion ; 2) Accelerated residual testing to predict future ultimate expansions that can be achieved in laboratory conditions; 3) Procedure to use the above as input data for a finite element simulation; and 4) Sample reports for each method. Part 1 has been completed, and Part 2 is nearly completed[6]. Parts 3 and 4 have just gotten underway.

WG-2: Numerical Benchmark/Round-Robin Analyses Lists about 12 simple problems (related to both materials and structures) to be analyzed by FEA codes for "validation". This report is complete and, to the best of our understanding, the P.I. is the only to have completed all analyses.

WG3: - Field Assessment and Monitoring The first part, dealing with NDE and written by Giannini, Jacobs and Rivard, is now complete. Currently, Courtois and Grimal (*Electricité de France*) will be

[6]Contributors: Canada-Laval-Fournier, Canada-Ottawa-Sanchez, France-IFSTTAR-LCPC-Martin, France-Toulouse-Sellier, Japan-Katayama, Spain-Torroja-Menendez, Switzerland-EMPA-Leeman, UK-Wood.

revising and upgrading the document to address field assessments.

WG4: Impacts of ASR on Hydraulic Structures and Nuclear Power Plants Problems and Research Needs. The initial version was written by Amberg (Lombardi, Switzerland) and Gocevski (HydroQuebec) for the hydro and nuclear fields, respectively. This document will be revised and edited by Grimmal (*Electricité de France*).

36 Our next annual meeting will be held May 21-22 at the Bureau of Reclamation in Denver (NRC staff is hereby invited).

37 The committee should wrap up its work in 2019.

2.3 Task 3: Finite Element Simulations

2.3.1 Task 3-A: Risk-Based Assessment of Shear Walls

38 OECD/NEA/CSNI has released a benchmark problem centered on a shear walls tested at the University of Toronto. Shear walls, Fig. 12, with and without AAR were tested. Results (load displacement curve) after a 260 days expansion were made available, and participants were requested to predict response at 1,000 days. By general consensus, the data provided by the University of Toronto were incomplete and questionable.

39 CU Boulder nevertheless participated in this exercise and spent a substantial (and unallocated) amount of time completing the exercise. The originality of the analysis was its probabilistic basis embedded into a comprehensive report. All other reports were deterministic.

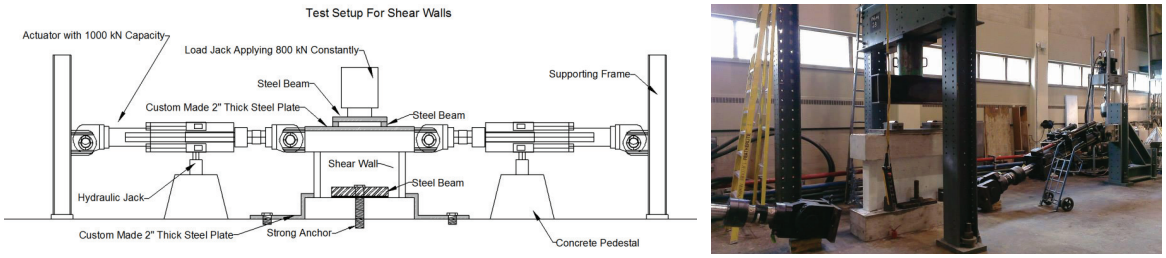

Figure 12: Test set-up for the shear wall

40 A preliminary deterministic analysis yielded the results shown in Fig. 13.

41 Prior to conducting a probabilistic analysis, a sensitivity analysis was performed. 15 potential variables were selected, each one assigned a probability distribution function, and 31 analyses were then performed. Sensitivities were then sorted, and these results are shown in the format of a so-called Tornado Diagram, Fig. 14(a). The corresponding prediction is displayed in Fig. 14(b)

42 Following the sensitivity analysis, of the 15 potential variables, only 5 were selected, and a Monte Carlo-based simulation with Latin-Hypercube sampling was carried out.

43 This step was achieved through a special software developed in-house that starts with a spreadsheet containing the variables and their distributions, then proceeds to generate the finite element meshes, runs the analyses, "data-mines" the output and ultimately produce the desired results.

44 A total of 100 analyses were performed, and the 16% and 84% fractile (corresponding to mean minus and mean plus one standard deviation) capacity curves were extracted, Fig. 14. Experimental results did indeed

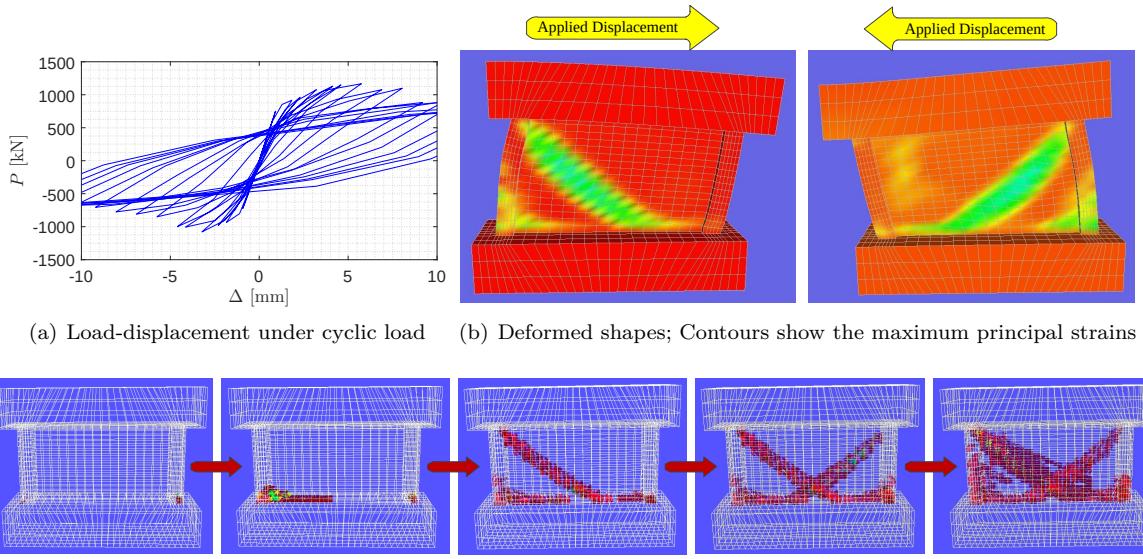

(a) Load-displacement under cyclic load (b) Deformed shapes; Contours show the maximum principal strains

(c) Crack propagation in web and columns

Figure 13: Structural response of shear wall under cyclic displacement (without ASR)

fall within the narrow limits.

45 This analysis has provided the framework allowing for subsequent risk-based assessments, similar to this one, to be easily performed.

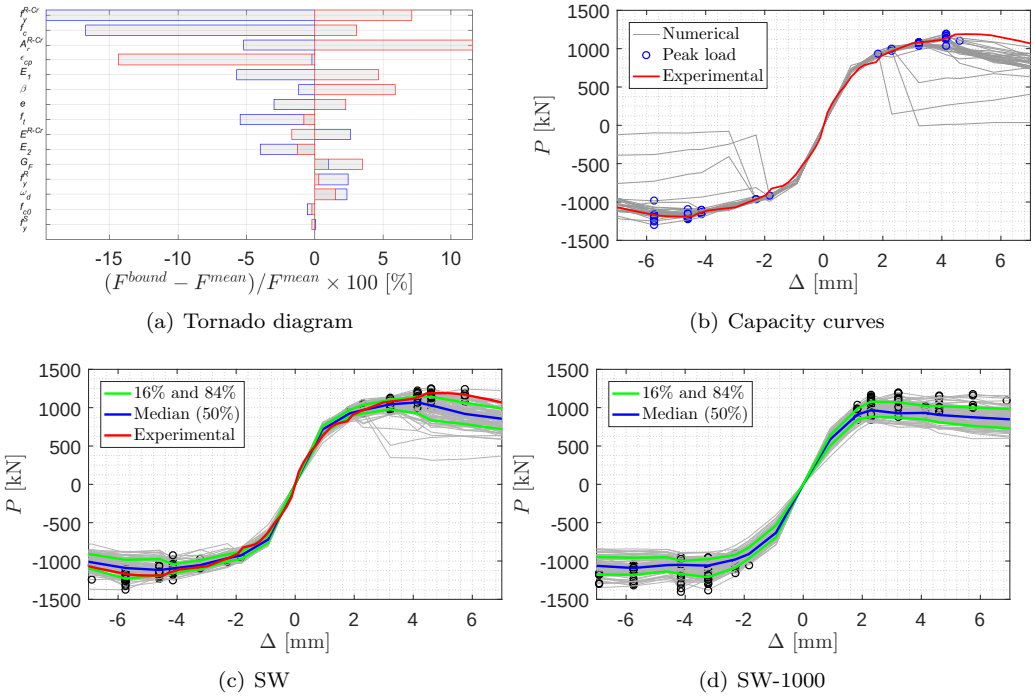

(a) Tornado diagram (b) Capacity curves

(c) SW (d) SW-1000

Figure 14: Results of shear wall analyses

2.3.2 Task 3-B: Risk Assessment of an NCVS Subjected to AAR and Seismic Excitation

46 One premise of this analysis is that AAR by itself will not jeopardize the structural integrity of an NCVS, at most its serviceability (through deterioration of the steel-concrete bond interface). On the other hand, AAR will degrade shear strength and thus may affect the resilience of the structure when subjected to lateral load (i.e. seismic excitation), especially since many NCVS are not fitted with shear reinforcement.

47 The report associated with this task is composed of two parts:

1. A very extensive coverage of the theories related to: AAR, nonlinear transient finite element analysis, seismic hazard analysis, and probabilistic-based analyses. To the best of our knowledge, this coverage is by far one the most extensive (more so than NUREG-1150).
2. Detailed 3D transient analysis of an NCVS subjected to 40 years of AAR expansion (up to 0.3%) and then subjected to seismic excitation.

. Following is a summary of the analysis.

48 The NCVS selected for our case study is heavily influenced by the one illustrated in NUREG-6706 and is schematically shown in Fig. 15(a).

49 Note that 56' of the total 122'-high cylindrical part is below grade and only the concrete underneath it will be subjected to AAR (as a result of the high RH likely to be present in the surrounding foundation). A reinforcement ratio of 0.5% was assumed for both the vertical and horizontal directions.

50 For the seismic study of the NCVS to be properly performed, radiation must be damped and the effects of rocking mitigated.

51 Radiation damping was mitigated by placing Lysmer dashpots (also known as "silent" boundary conditions) at the end of the foundation.

52 Rocking is caused by the eccentricity of the center of mass, which is subjected to the lateral inertial force. Rocking (seldom addressed in published reports) affects the soil-structure interaction by potentially uplifting the base from the rock (especially if vertical excitation has been taken into account) and opening a gap between the structure and the adjacent rock. This phenomenon was mitigated by inserting zero-thickness joint elements around the container (and below it).

53 Another parasitic effect of rocking is the "hammering" of the base, which occurs along with a (nearly) linear uplifting of the foundation base. This effect was mitigated by first performing a static analysis with rigid vertical supports at the base and then (with the internal strains/stresses "locked in") restarting initiation of the transient analysis. In this second analysis however, the supports are removed and the reactions are substituted by corresponding vertical forces (equal to the reactions). Thus the structure has no support whatsoever (only possible in dynamic analyses).

54 An analysis was performed using the Merlin finite element code, with the models shown in Figure 15(b). The NCVS is 37 m high, has a base mat 3.0 m thick and an internal radius of 19.0 m. Potential separation due to rocking is shown in Fig. 15(c), and the foundation dimensions are given in Fig. 15(d). Also displayed in these figures are the 15 different color-coded material groups described in the next section.

55 Essentially, this analysis seeks to first simulate 40 years of slow AAR expansion, followed by a few seconds of intense seismic lateral excitation, Fig. 16(a). The imposed AAR was a moderate 0.3% volumetric

expansion accumulated over 40 years, Fig. 16(b). Lastly, a synthetic ground motion of linearly increasing intensity was applied, Fig. 16(c) (six different accelerograms were actually applied).

56 The technique of applying relatively few linearly increasing accelerations is known as Endurance Time Analysis Functions (ETAF).

57 A preliminary analysis (as described above) was performed under the assumption of the absence of AAR. Results will be contrasted with this baseline.

58 The structural response of the NCVS subjected to AAR only (Static + AAR) is shown in Fig. 17. Note the impact of using joint elements at the base and around the vessel to allow for potential (hidden) "delamination" between the base mat and foundation.

59 The impact of AAR on the structural response of an NCVS can now be ascertained by comparing Static + Seismic and Static + AAR + Seismic for:

Displacements: The absolute values of the (horizontal) displacements corresponding to peaks in (the six)

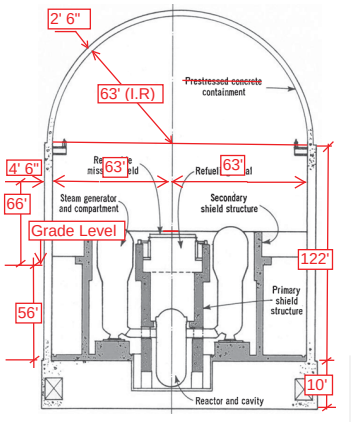

(a) Cross-section and geometry

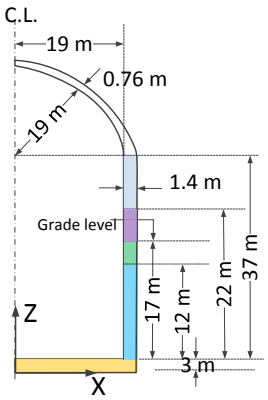

(b) Detailed geometry

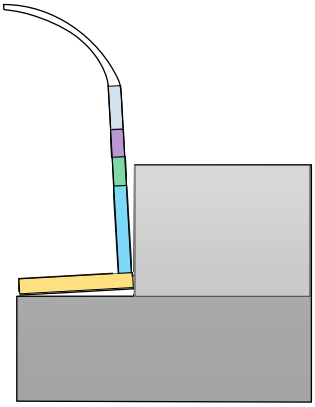

(c) Potential rocking and ensuing separation of container from foundation

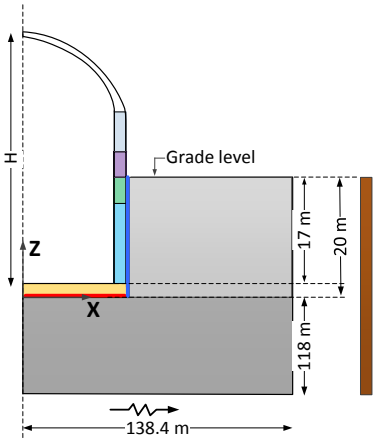

Location	Mesh Density	Material Group	AAR
Base	Coarse	1	Y
Wall Below Grade	Coarse	2	Y
Wall Below Grade	Fine	2	Y
Wall Above Grade	Fine	3	N
Wall Above Grade	Coarse	3	N
Dome	Coarse	4, [5]	N
Foundation	Coarse	6	N
Lateral Rock	Coarse	7	N
Base Interface Elem.	-	8, 10	N
Side Interface Elem.	-	9, 11	N
Reinforcement (V)	-	12	N
Reinforcement (H)	-	13	N
Viscous Damper	Coarse	14, 15	N

(d) Model and accompanying material groups

Figure 15: Geometry and model idealization

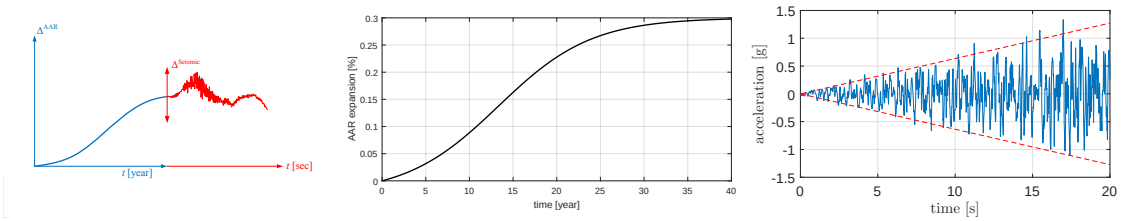

(a) Schematic representation of the analysis (b) Imposed AAR expansion model (c) ETAF accelerogram

Figure 16: Loads imposed on the NCVS analysis

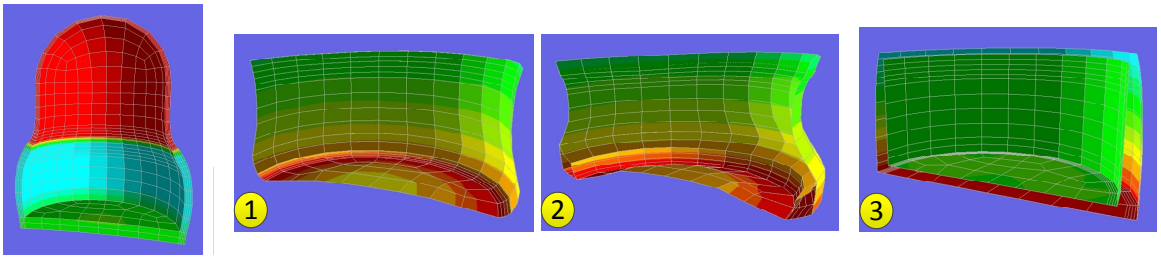

(a) Swelling of the contaminated zone (b) Evolution of joint opening/sliding due to AAR

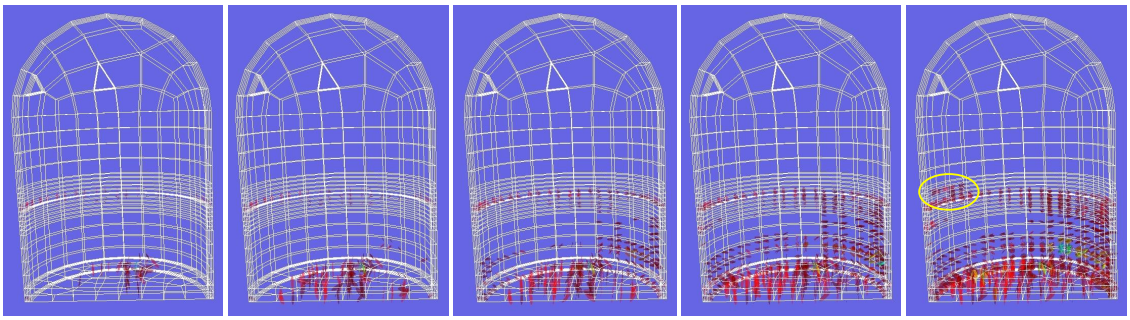

(c) Internal cracking

Figure 17: Response of NPP under an AAR analysis

ETAF cases are shown in Fig. 18(a). This is a ramping curve since the ground acceleration is indeed defined as linearly increasing (Fig. 16(c)). Three sets of results are indicated, namely:

1. Ground motion without AAR
2. AAR with accompanying material degradation followed by ground motion.
3. AAR without material degradation followed by ground motion.

To better determine the impact of AAR, the responses have been normalized with respect to the analysis without AAR (i.e. ground motion only), Fig. 18(b).

It should be noted that the displacements are all plotted as ETA functions (expression of the maximum absolute values of EDP during the time interval from 0 to t, in terms of time). Hence, an ETA function increases over time in an engineering demand parameter (EDP-time coordinate system). Failure in this function corresponds to a (semi-) vertical line at $t = t_{\text{failure}}$.

Stresses The histograms of maximum principal stresses are shown in Fig. 19 for various locations. Results are presented for ground motion only without AAR (in blue), and AAR (with degradation) followed

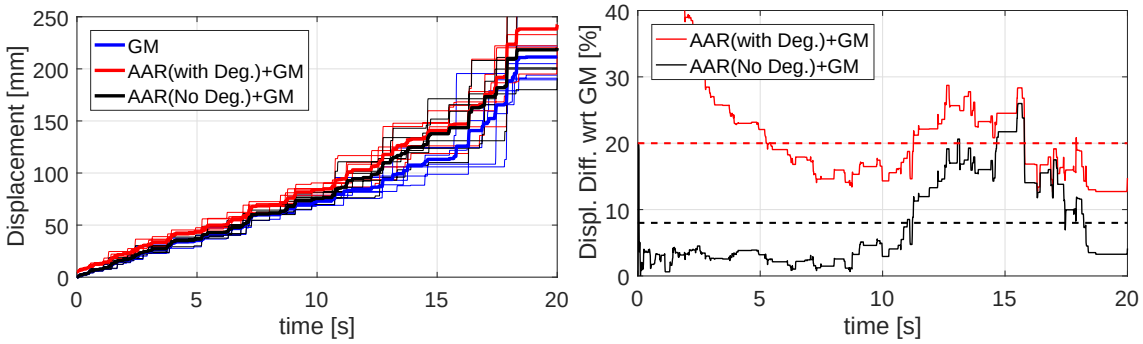

(a) Displacement profile at the top

(b) Normalized displacements and mean differences

Figure 18: Response of NCVS under AAR and seismic

by ground motion.

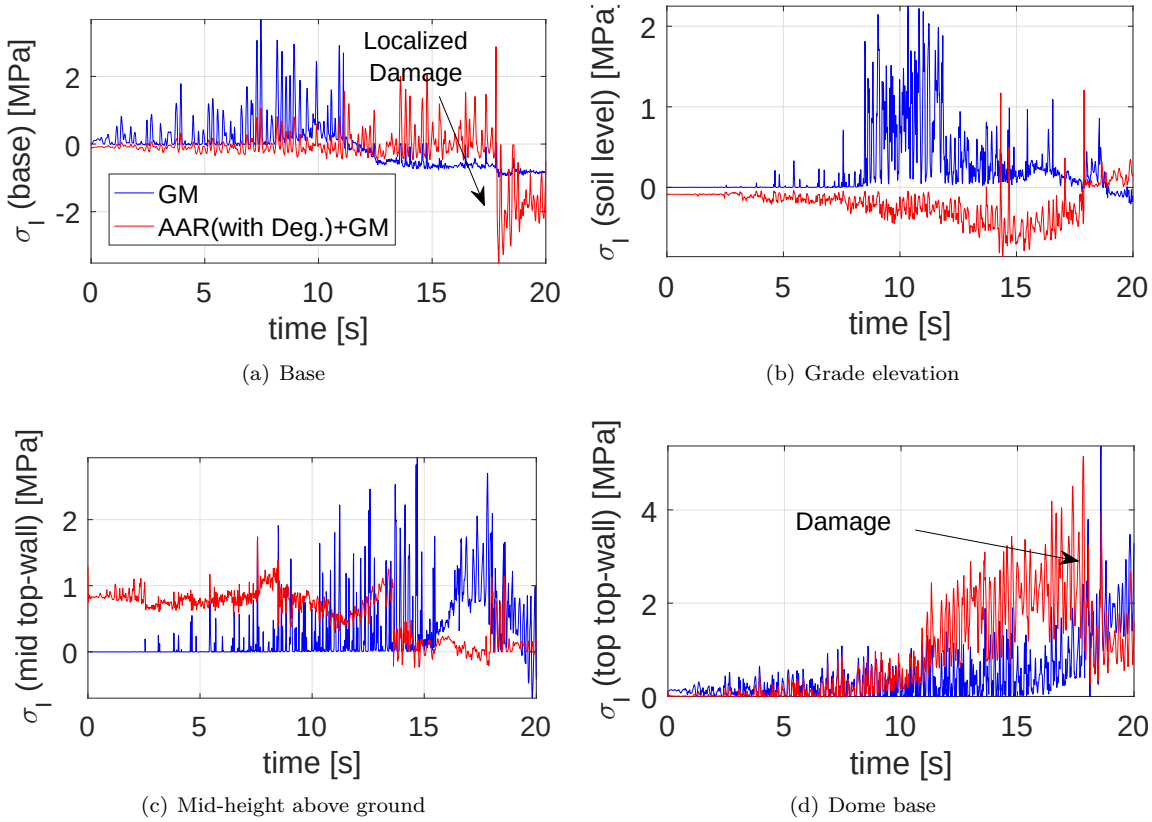

(a) Base

(b) Grade elevation

(c) Mid-height above ground

(d) Dome base

Figure 19: Principal stress-time histories from the seismic analysis

Cracking of the structure is shown in Fig. 20.

From the previous figures summarizing results, the following observations can be offered:

1. AAR (with material degradation) will soften the concrete, thus resulting in smaller lateral displacements.
2. If material degradation is ignored (which is an erroneous abstraction), displacements will still be

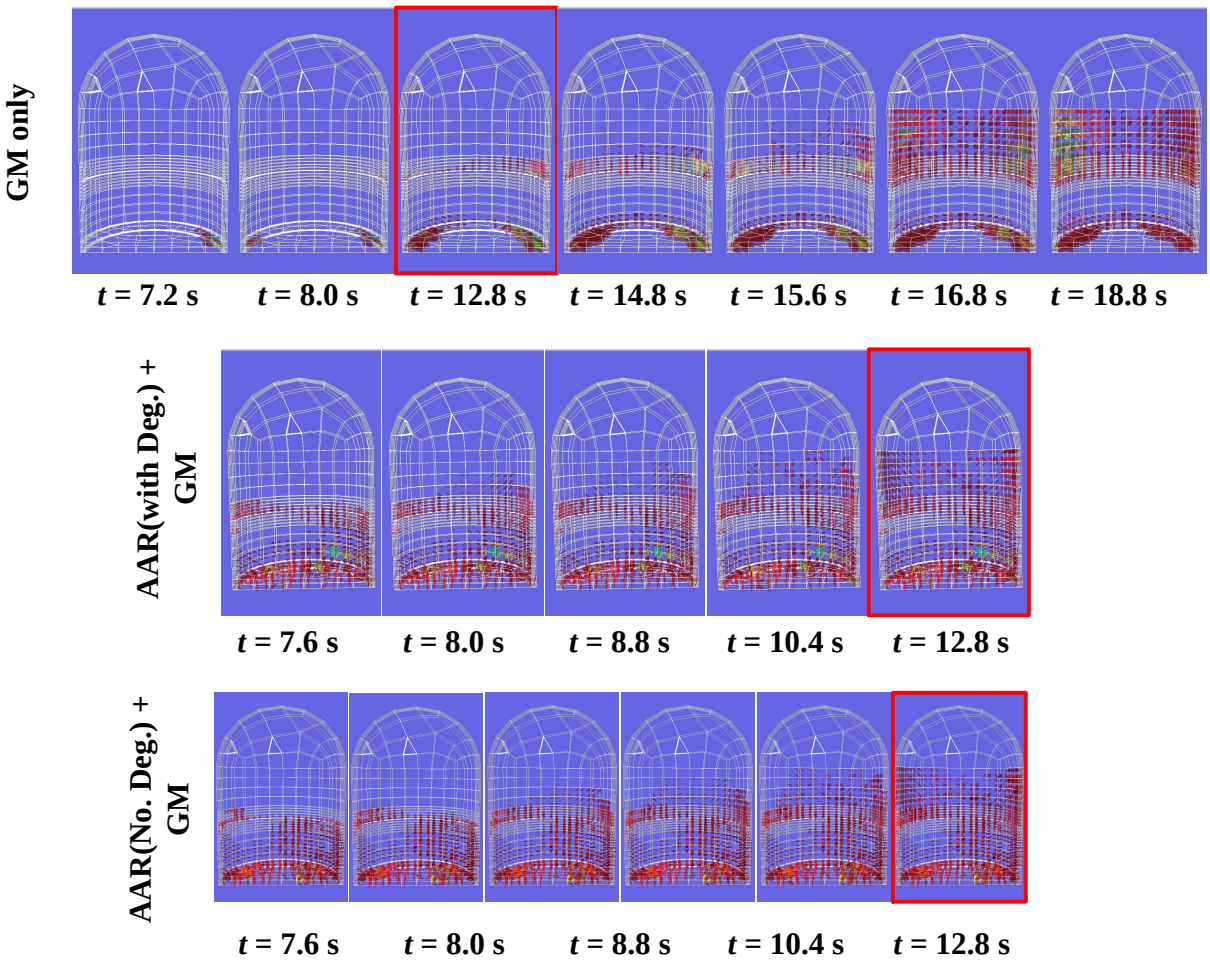

Figure 20: Crack profile from seismic analysis

smaller than cases without AAR, but larger than AAR with degradation. Note that the discrepancy with respect to the case without AAR starts at around 9 sec (i.e. until this point, the AAR had little impact on deformation).

3. The impact of AAR (with and without degradation) is time-dependent due to the complexities of the internal stress states induced by AAR or resulting from the seismic excitation, Fig. 18(b). On average and for this case study, AAR with degradation results in a 20% change, whereas the case without degradation only yields an 8% variation with respect to the "GM" model.
4. The principal maximum stress history profile at various locations, Fig. 19, reveals that additional damage will be induced by AAR (with internal damage being taken into account).
   (a) At the base, Fig. 19(a), maximum principal stresses are indeed positive and attenuate with time. At first, stresses are lower in the presence of AAR expansion, but then suddenly increase with a localized damage at time $\sim$ 17 sec.
   (b) At the grade elevation, stresses are much higher without AAR, and then gradually decrease with no indication of failure. Note that the tensile strength equals 3.1 MPa. On the other hand, in the presence of prior AAR expansion, the stresses are negative, and a sudden localized failure appears at t= 14 sec.

(c) For a point above grade, stresses are higher in the absence of AAR, and there is an indication of localized failure at $t = 15$ sec. In the presence of AAR, this failure is delayed to about 17 sec.

(d) At the base of the dome, the AAR stresses are substantially higher than with stresses absent, and localized failure occurs around 17 sec.

5. For this case, AAR has reduced stresses at the base but substantially increased them at the base of the dome.
6. The previous observations are qualitatively confirmed by the crack profiles shown in Fig. 20. Indeed, the damage index (DI), i.e. the ratio of cracked cross-sections to total area, is highest when AAR (with damage) has preceded the seismic expansion.
7. The AAR has a much greater impact on the portion of NCVS below grade than on that above grade (where no AAR has been modeled).

3 Synthesis and Conclusion

61 To the best of our knowledge, this study is the most comprehensive on the effect of AAR on the shear strength of concrete.

62 16 large specimens were carefully prepared and tested using a unique apparatus designed for shear testing. It was determined that a 0.6% expansion reduces strength by 20%.

63 For this particular study, AAR (a relatively low 0.3%) reduced the resilience of an NCVS subjected to seismic excitation by approximately 20%.

64 It should also be noted that this reduction, associated with a 0.3% localized uniform expansion, is roughly equal to the reduction in shear strength experimentally observed for expansions of about 0.6

65 Our results imply that a material shear strength degradation of x % will have a larger percentual impact on the displacements and stresses when used in the nonlinear seismic analysis of a NCVS. In our study the material degradation was $\sim$ 20% corresponding to an AAR of $\sim$ 0.6%, whereas the finite analysis had a $\sim$ 20% degradation for an AAR of 0.3%.

66 Through the validated finite element code, parametric studies for different combinations could be conducted with a reasonable level of confidence.

4 Recommendations for Future Work

67 When such an extensive investigation is performed, invariably some points are found to require further clarification. These fall into two categories: desirable and critical.

Desirable topics include:

Numerical Repeat the finite element analysis:

1. Include a random distribution of the AAR-contaminated concrete so as to better reflect an actual case.
2. Include deconvolution, and possibly free-field attenuation of the excitation record.
3. Stochastic analysis resulting in fragility curves

Experimental tests to include:

1. A more detailed experiment to study the effects of temperature, size and reinforcement on ASR expansion in concrete.

2. Study of the transition from accelerated laboratory tests (under constant high temperature and relative humidity) to an actual structure subjected to (typically lower) variable temperature and relative humidity.
3. Further study size effects, a greater number of specimens gradually increasing in size would be needed to derive a more definitive statement regarding its effect.

Critical Based on the P.I.'s past experience with dynamic testing[7], Fig. 21(c), concrete exhibits a strength *increase* when subjected to a dynamic load. The P.I., in using a relatively unique facility at the University of Colorado (a set of three dynamic actuators controlled by custom software), Fig. 21(a) showed that for the columns tested, a 30% increase in strength was achieved. Accordingly, the test set-up laid out in Fig. 21(b) is highly recommended, but only if seeking to (partially) circumvent the deleterious effect of AAR on the shear strength of an NCVS subjected to seismic excitation (careful, as the failure mode may shift with a stronger concrete).

[7]Not to be confused with slow reverse cyclic loading that some, very erroneously, label as a seismic load.

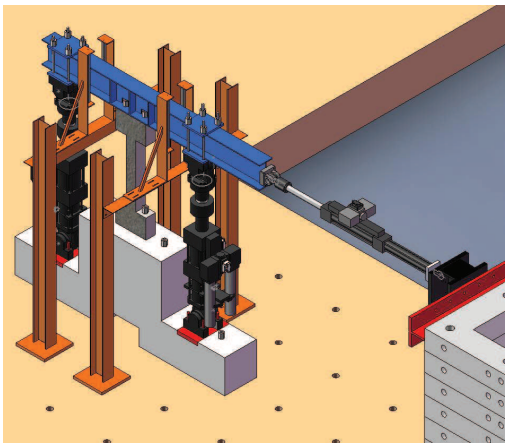

(a) Experimental set-up: constant vertical force, zero top rotation, dynamic lateral displacement

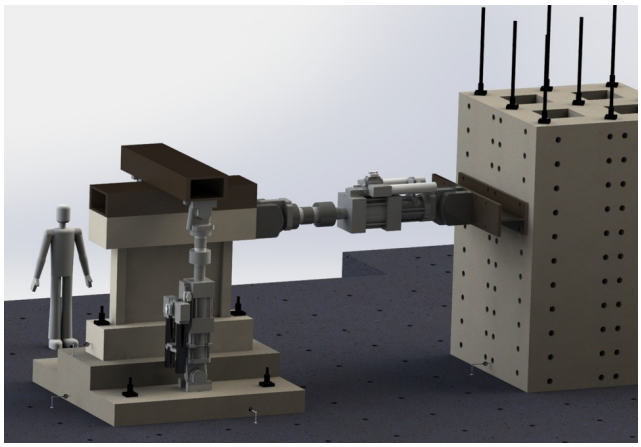

(b) Proposed test set-up

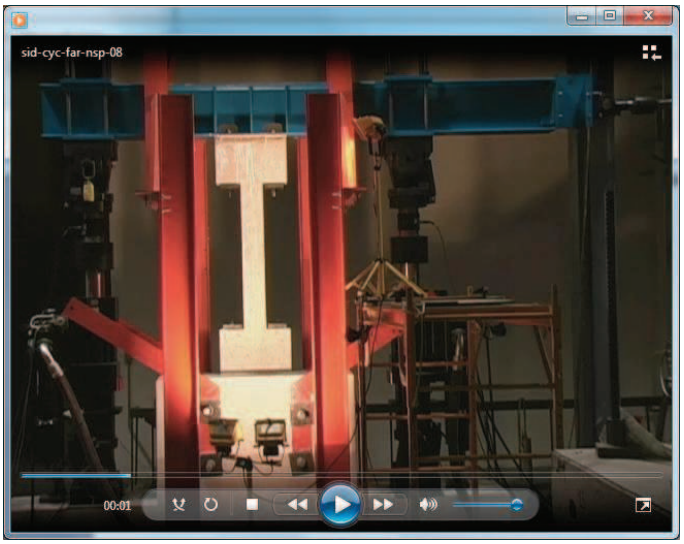

(c) Dynamic tests performed by the P.I.. To activate video: 1. Click on image; 2. When prompted by `Options`, select `Trust this document always`; 3. Click again on the image

Figure 21: Dynamic testing